Supplementary Information

The Effects of Irradiation on Structure and Leaching of Pure and Doped Thin-Film Ceria SIMFUEL Models Prepared via Polymer-Templated Deposition

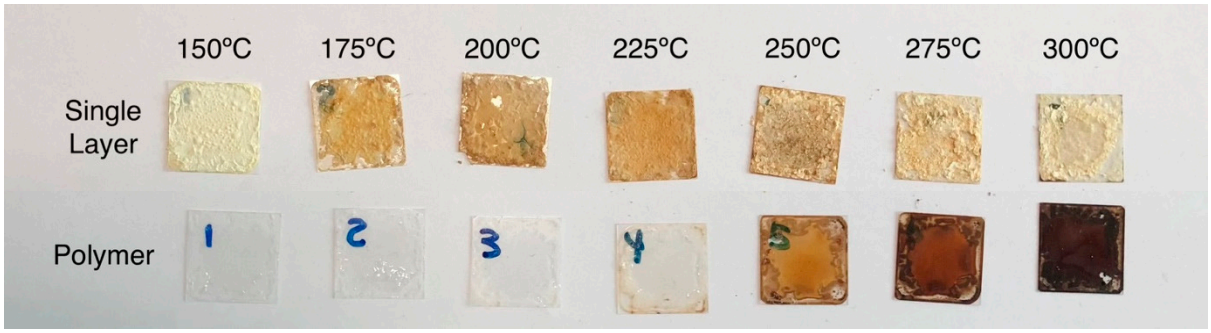

Figure S1. Effect of calcination temperature on deposited template and CeO_2 films calcined under air for 30 mins. Above 200 °C, breakdown of the polymer template is observed alongside the onset of frangibility in the CeO_2.

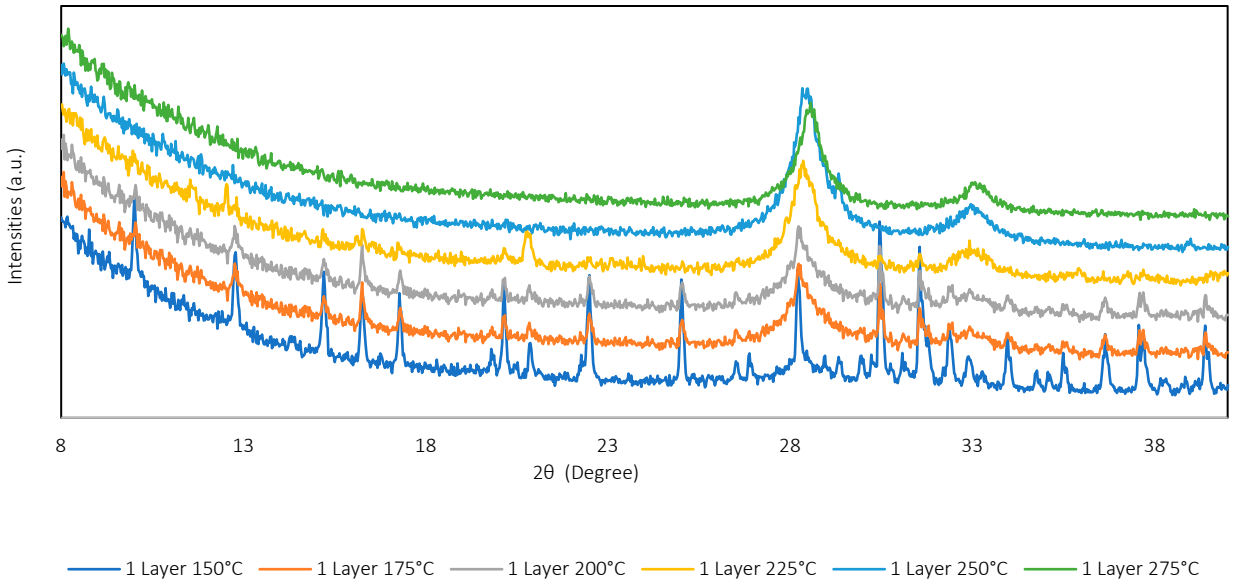

Figure S2. XRD diffraction patterns of films calcined at different temperatures for 30 mins, as outlined in **Figure S1**. The CeO_2 phase is beginning to form by 200 °C, and hence a longer calcination period at this temperature was selected.

TGA/DTA analysis of the dried (4 g/L) PDDA/PMAA template, evaporated CAN solution (0.1 M), and a 50:50 mixture by precursor volume of these two components was conducted under air, with the mass loss and rate of mass loss curves shown in **Figure S3a** and **S3b** respectively. Additionally, differential mass analysis, allowing for the quantification of negative or positive interactions between the CAN and polymer template was also conducted, as shown in **Figure S4**. The data points for this were calculated as per **Equation 2** [1–3], adjusting the calculated TGA curve for the mass ratios of the components within the system.

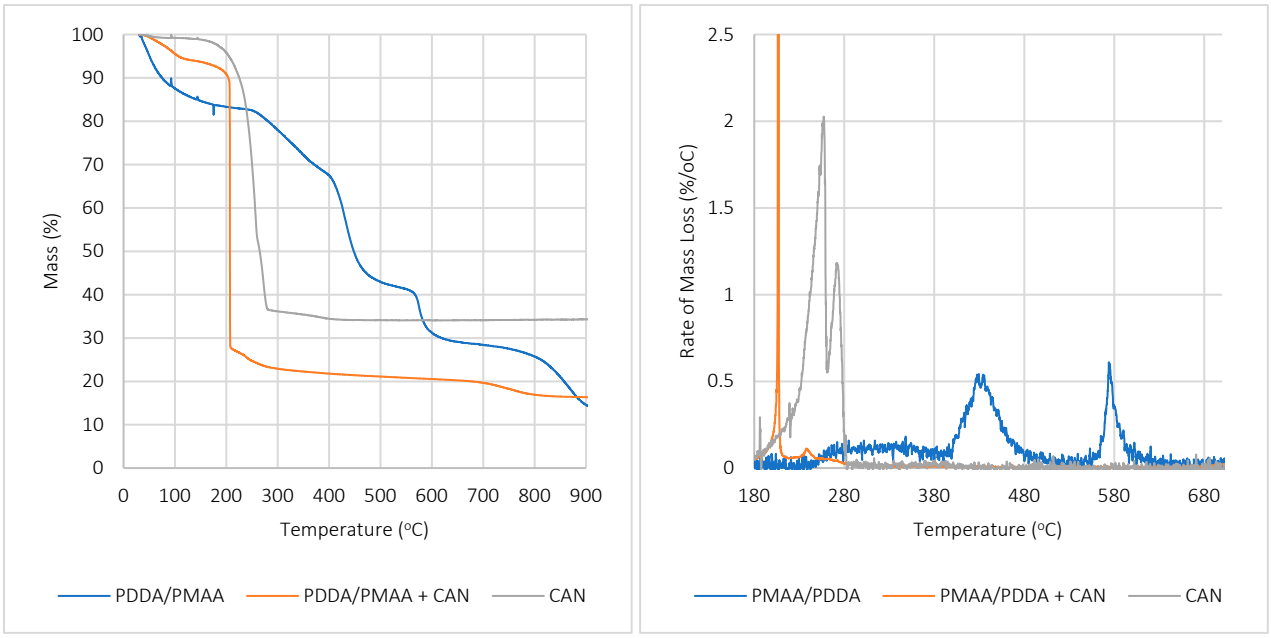

(a) (b)

Figure S3: Mass loss curves (a), and rates of mass loss (b) for PDDA/PMAA polymer template, a combined sample, and CAN, as deposited. 100 mL.min^{-1} air, 10 °C.min^{-1}, ambient to 1000 °C. The peak mass loss rate of the combined sample is 114 wt%.°C^{-1}. The associated heat flows accompanying these figures are presented in **Figure S5**.

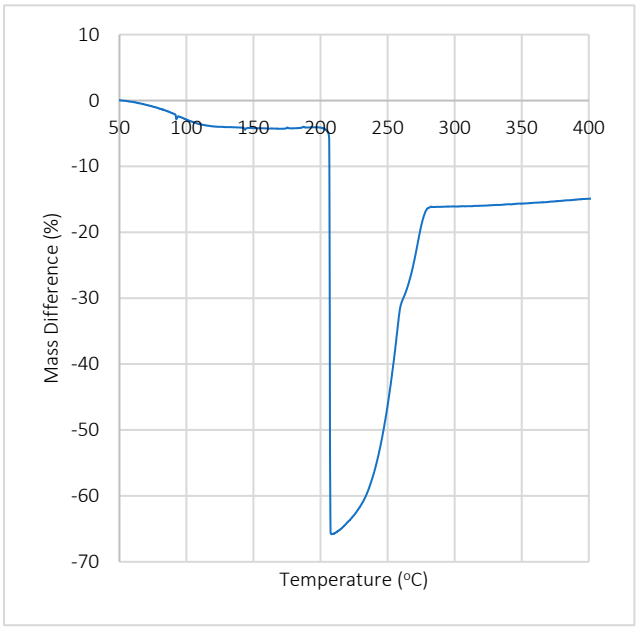

Figure S4. Differential mass graph for the recorded TGA results, calculated as previously described. [1-3].

The degradation of the PMAA/PDDA template behaves in a similar way to the two separate components [4,5], and the small residue remaining at 1000 °C is likely NaCl. The PMAA/PDDA template is stable to 240 °C with no discernible mass loss following the loss of water by 200 °C. The onset of CAN degradation as measured here is *ca* 180 °C combined with a two-stage mass loss with peak rates of mass loss at 258 and 276 °C respectively, mirroring the work of Audebrand [6]. Any differences in thermogravimetric response are due to the differences in sample preparation between this prior work and that presented here.

When combined, however, the thermal degradation of the PMAA/PDDA-CAN system is significantly altered, as illustrated by the large negative response shown in **Figure S4**. This illustrates a rapid evolution of volatiles at 207 °C, representing 66% of the mass if no interaction between the two components occurred. This coincides with a large DSC exotherm at the same temperature (see **Figure S1**). We can attribute this to a strong oxidative interaction between the Ce^{4+} centres and/or nitrate functionalities of CAN and the polymer template, producing volatiles such as CO_2 (from oxidation of carboxylate functionalities) [5,7], and NO_x (from nitrate decomposition), though confirmation of this would require TGA-FTIR, TGA-MS, or similar combinatorial analysis. This process likely mirrors the reactions intentionally utilised in nanoparticles combustion synthesis [7]. Above 280 °C, following the accelerated degradation observed in the combined sample, the observed mass is *ca* 15 wt% lower than would be expected in the absence of interactions. Thus, we can deduce that a sensible maximum calcination temperature for our films is 200 °C in this system to avoid undesired oxidation of the polymer template.

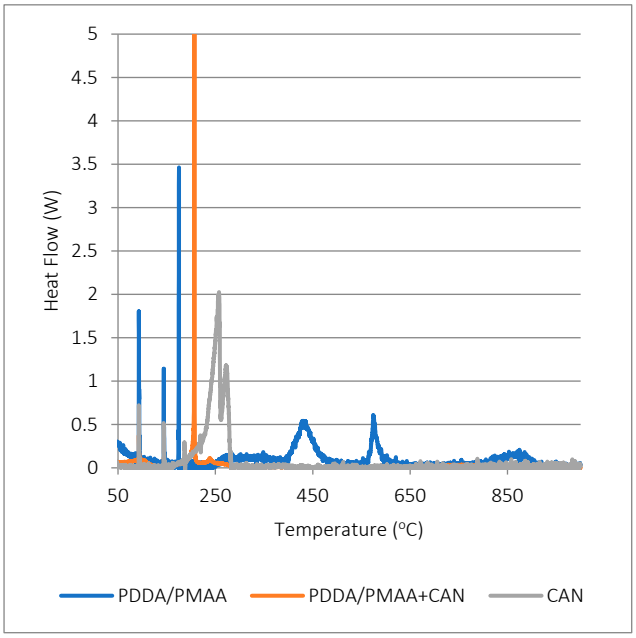

Figure S5. Heat flow of TGA data presented in **Figure S3**.

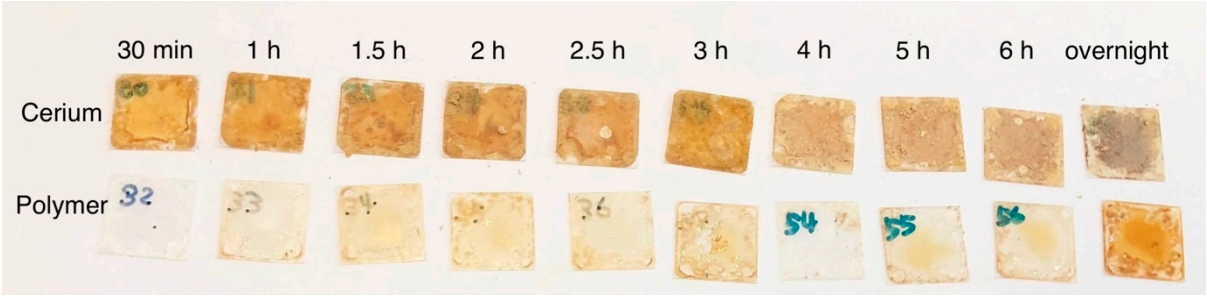

Figure S6. Photograph of slides after heating with varying time at 200 °C.

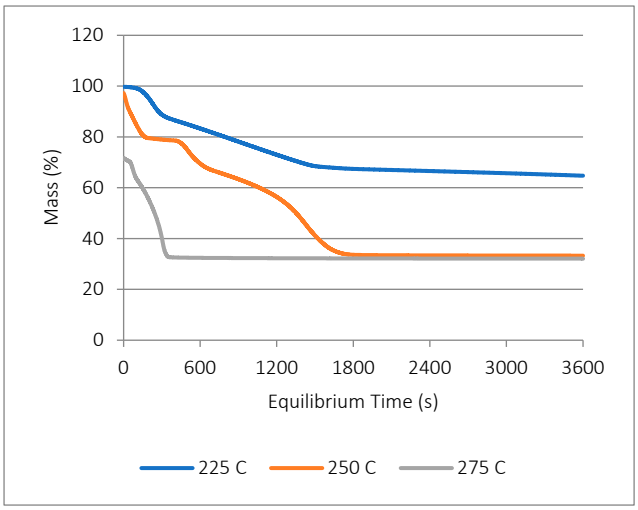

Figure S7. Variation in mass loss over time for pure CAN crystals held isothermally at a fixed temperature.

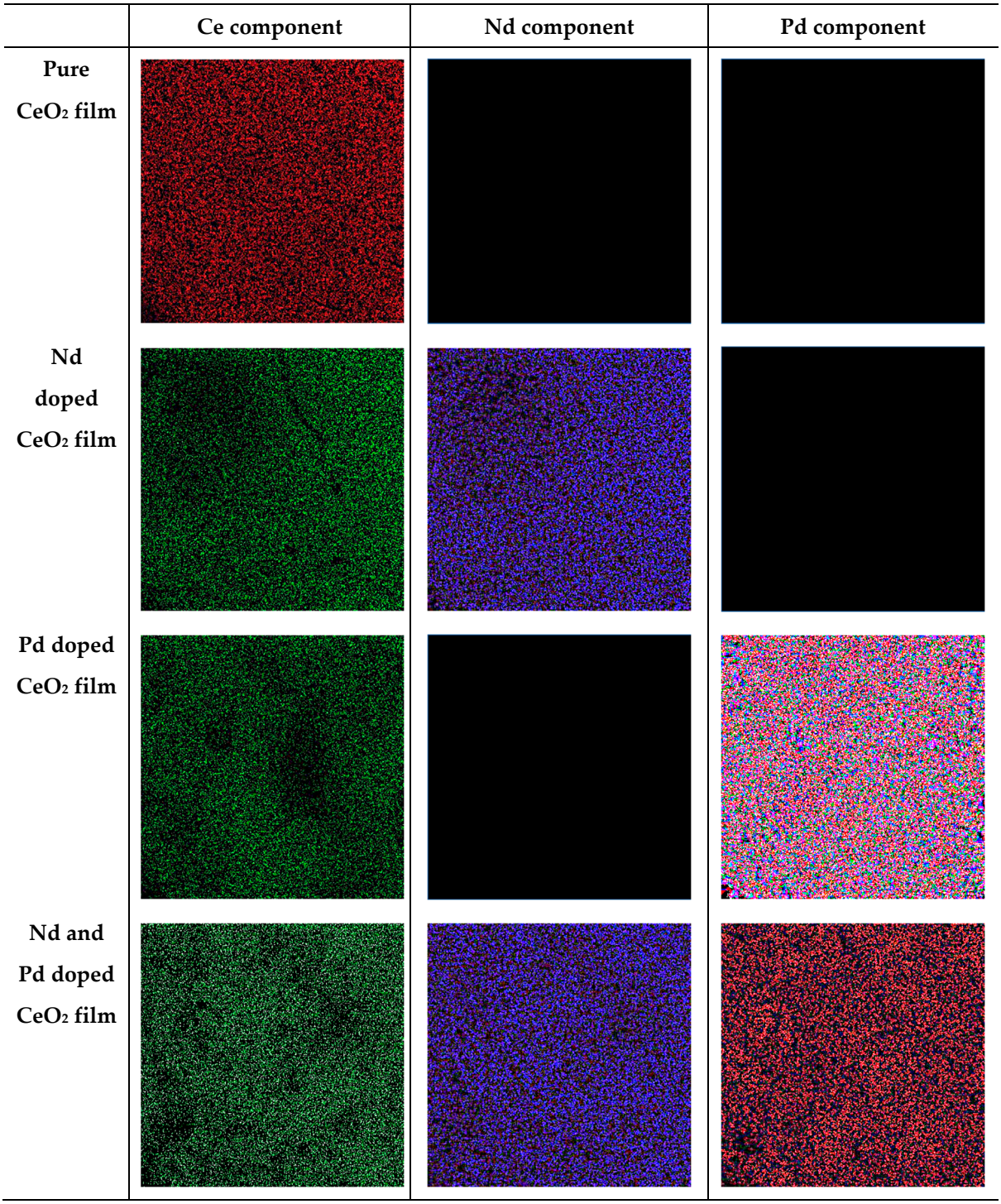

Figure S8. Elemental maps of pure CeO_2, Nd, Pd, and Nd+Pd-doped films. The Eu-doped films were similarly homogenous. Full image width represents wide zoom of film surface – of the order of mm.

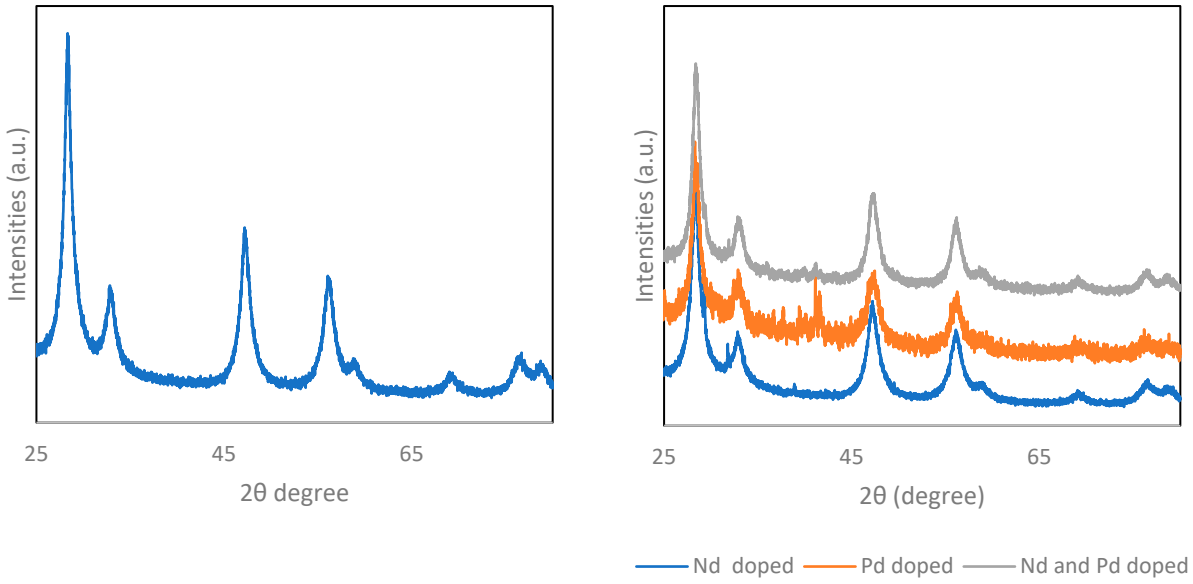

(a) (b)

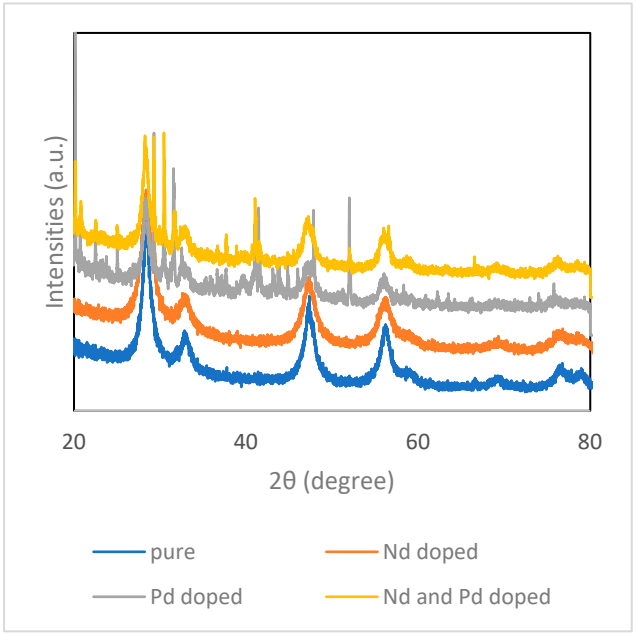

(c)

Figure S9. XRD Patterns of virgin (a – CeO_2 and b – Nd, Pd, and Nd+Pd-doped) and irradiated (c) CeO_2 films. Pd elemental response visible (grey and yellow trace). Pd response increases upon irradiation.

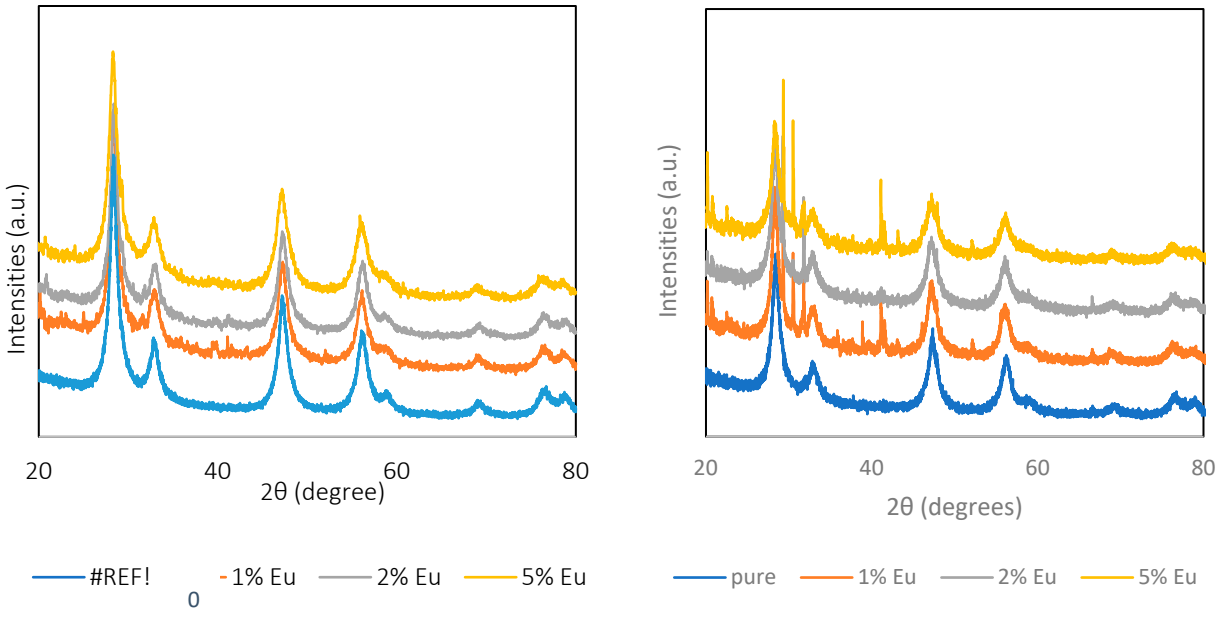

(a) (b)

Figure S10. XRD Patterns of virgin (a) and irradiated (b) pure and Eu-doped CeO_2 films. Note formation of nitratine ($NaNO_3$) irradiation for 1% and 5% samples.

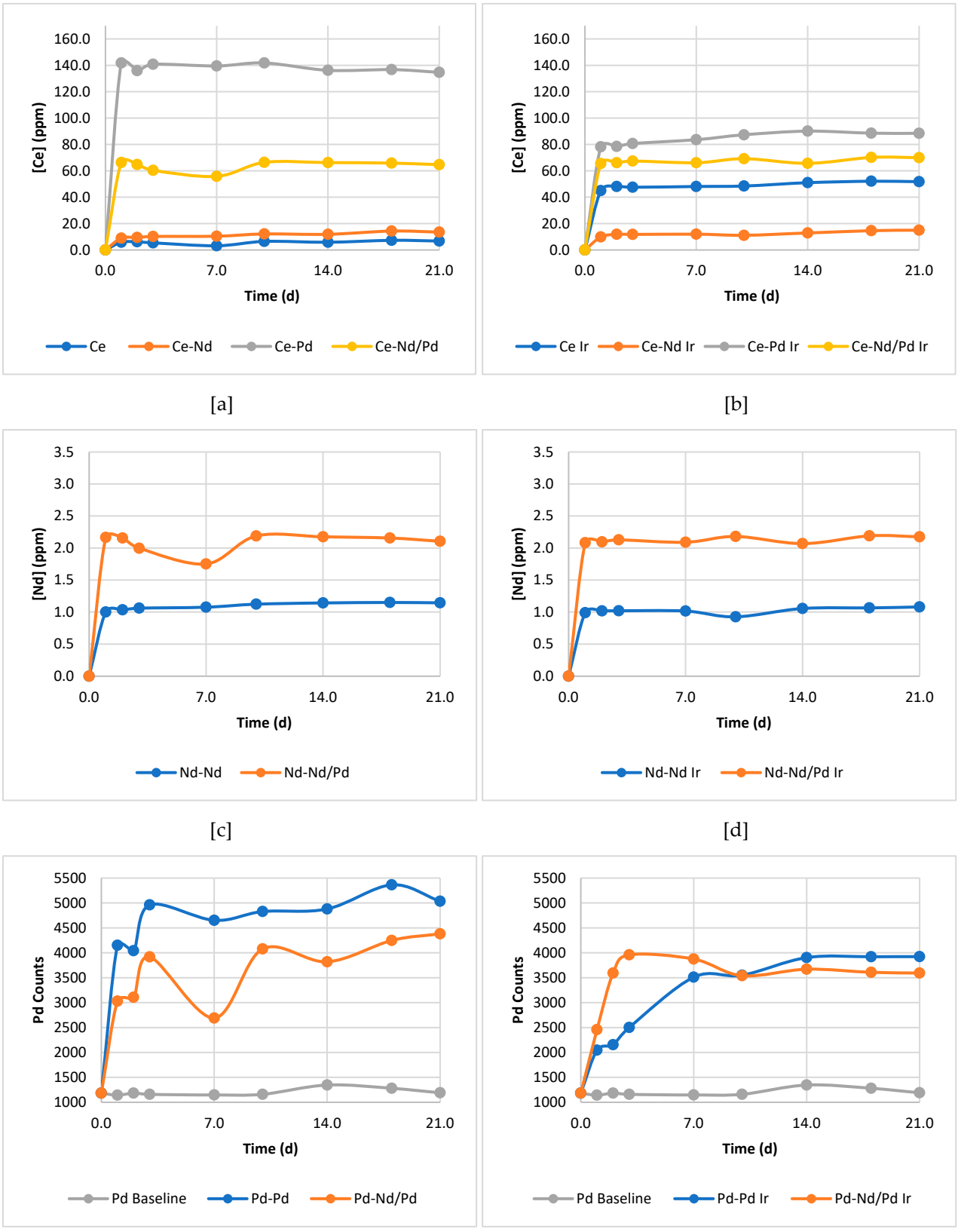

Figure S11. Ce (a and b), Nd (c and d), and Pd (e and f) leaching over time in Ce-Nd-Pd sample matrix. Virgin (a, c, e) and irradiated (Ir, b, d, f). The y-axis is scaled to the maximum concentration possible for each metal. 100% Ce: 168.13 ppm; 2% Nd: 3.46 ppm.

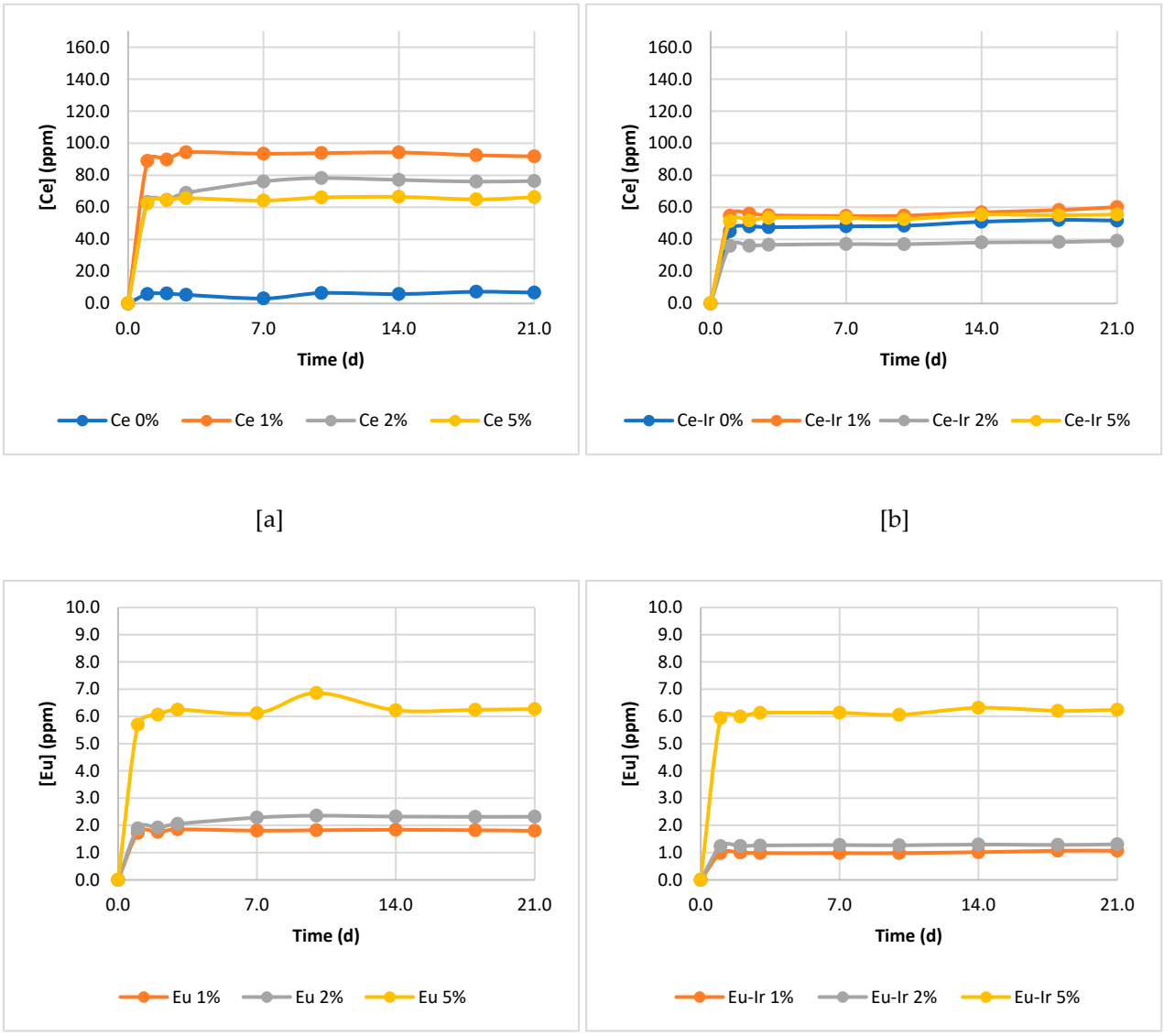

[a] [b]

[c] [d]

Figure S12. Ce (a and b), and Eu (c and d), leaching over time in Ce-Eu sample matrix. Virgin (a, c) and irradiated (b, d). The y-axis is scaled to the maximum concentration possible for each metal. Ce: 168.13 ppm; 1% Eu: 1.82 ppm; 2% Eu: 3.65 ppm; 5% Eu: 9.12 ppm.

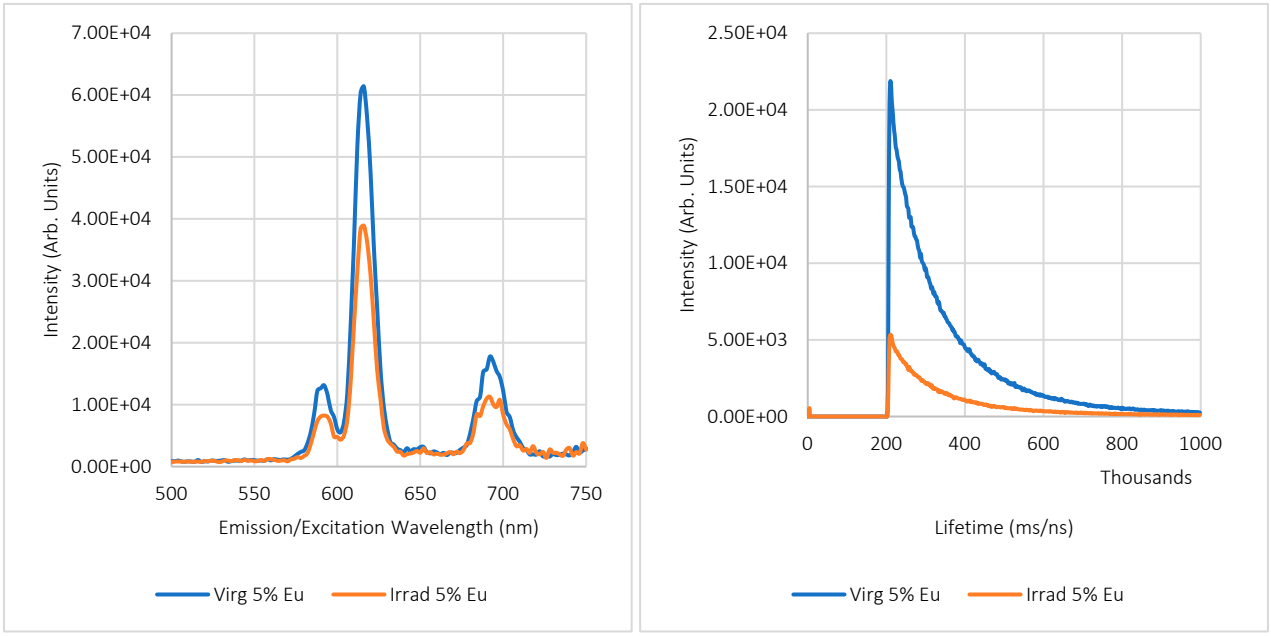

[a] [b]

Figure S13. TRLFS spectra of 5% Eu-doped virgin and irradiated CeO_2 films (a) with Eu lifetime (b).

References

[1] Holdsworth, A.F.; Horrocks, A.R.; Kandola, B.K.; Price, D. The potential of metal oxalates as novel flame retardants and synergists for engineering polymers. *Polym. Degrad. Stab.* **2014**, *110*, 290–297. https://doi.org/10.1016/j.polymdegradstab.2014.09.007.

[2] Holdsworth, A.F.; Horrocks, A.R.; Kandola, B.K. Synthesis and thermal analytical screening of metal complexes as potential novel fire retardants in polyamide 6.6. *Polym. Degrad. Stab.* **2017**, *144*, 420–433. https://doi.org/10.1016/j.polymdegradstab.2017.09.002.

[3] Holdsworth, A.F. Novel Metal Complex Fire Retardants for Engineering Polymers. Ph.D. Thesis, University of Bolton, Bolton, UK, 2015.

[4] Pont, A.-L.; Marcilla, R.; De Meatza, I.; Grande, H.; Mecerreyes, D. Pyrrolidinium-based polymeric ionic liquids as mechanically and electrochemically stable polymer electrolytes. *J. Power Sources* **2009**, *188*, 558–563. https://doi.org/10.1016/j.jpowsour.2008.11.115.

[5] Schild, H.G. Thermal degradation of poly(methacrylic acid): Further studies applying TGA/FTIR. *J. Polym. Sci. A* **1993**, *31*, 2403–2405. https://doi.org/10.1002/pola.1993.080310925.

[6] Audebrand, N.; Guillou, N.; Auffrédic, J.P.; Louër, D. The thermal behaviour of ceric ammonium nitrate studied by temperature-dependent X-ray powder diffraction. *Thermochim. Acta* **1996**, *286*, 83–87. https://doi.org/10.1016/0040-6031(96)02944-9.

[7] Purohit, R.D.; Saha, S.; Tyagi, A.K. Nanocrystalline Ceria Powders Through Citrate–Nitrate Combustion. *J. Nanosci. Nanotechnol.* **2006**, *6*, 209–214. https://doi.org/10.1166/jnn.2006.17932.